Journal of Engineering Science and Technology
Vol. 12, No. 11 (2017) 2855 - 2865

APPLICATION OF TAGUCHI TECHNIQUES TO STUDY DRY SLIDING WEAR BEHAVIOUR OF MAGNESIUM MATRIX COMPOSITES REINFORCED WITH ALUMINA NANO PARTICLES

TARASASANKA C.*, RAVINDRA K.

Department of Mechanical Engineering, R.V.R & J.C College of Engineering, Guntur, India
*Corresponding Author: tarasasankac@gmail.com

Abstract

Magnesium metal matrix composites reinforced with alumina Nano particles are prepared by liquid metallurgy route. Dry sliding wear behavior of the composite was tested and compared with AZ91 magnesium alloy. A design of experiments based on Taguchi technique is used to acquire the data in a controlled way. An L9 orthogonal array is employed to trace out the influence of wear parameters like Sliding Speed, Applied Load, Sliding Distance and Percentage of reinforcement on dry sliding wear of the composites. Objective of the model was chosen as "smaller the better" characteristics to analyse the dry sliding wear behaviour. Results show that sliding distance has the highest influence on wear and load is predominant factor on the response of friction. The mathematical model was developed using regression analysis to determine the wear and friction force of composites.

Keywords: Dry sliding wear, Taguchi technique, Magnesium alloy.

1. Introduction

The rapid, significant development evolved necessity to search for new multipurpose full developed technology in the manufacturing quality of product, not only at the minimization of dimensions and mass but also growth in its reliability and dimensional stability in working conditions. As the present technology intends for light vehicle constructions as possible and expects for low fuel consumption by using magnesium alloys as a material in case of car wheels, engine pistons, gearbox and clutch housings, framing of doors, pedals, manifolds, housings of propeller shafts, differential gears, brackets, radiators and others.

Nomenclatures

A,b1…b4, c1…c4	Constants
D	Sliding Distance, m
FF	Friction Force, N
L	Load, N
R	Percentage of reinforcement, %
S	Sliding Speed, m/sec
S/N ratio	Signal to Noise ratio
W	Wear, µm
µ	Mean
σ	Standard Deviation

Abbreviations

EDM	Electric Discharge Machine
HRC	Rockwell Hardness 'C' Scale.
SEM	Scanning Electron Microscope

Alloys can produce qualitative products as they are expensive. Even then the customers prefer to the purchase of alloy materials. Usually magnesium and its alloys are used in motor industry and machine building. In fact, they also go with applications in helicopter production, planes, air navigation, chemical and nuclear power industries [1].

Actually aluminium and zirconium are main alloying elements of magnesium alloys. AM and AZ series of Mg-Al based alloys provide great stiffness and strength at room temperature and not suitable for service at temperatures of 150-200^{0}C since they exhibit low creep strength. Many alloying elements have an influence of mechanical, physical and chemical properties. From Fig. 5 and table 4 load is a dominant parameter on the frictional force and from Fig. 6 and Table 5 Sliding distance is a dominant parameter on the wear. Based on discussions it is also evident from tables that the optimum conditions for wear are *S*: 3m/sec; *L*: 20N; *D*: 1500 m and percentage of reinforcement: 3%. Similarly the optimum conditions for frictional force are S: 1m/sec; *L*: 20N; *D*: 1500 m and percentage of reinforcement: 3%.

For example aluminium maintains significant tensile strength.

The problems that we can face in many engineering applications is "wear" that effects the mechanical functioning of engineering parts by destroying the surface finish and reducing the fine tolerances. [2].

Many studies have been done in getting an idea on the wear behaviour of magnesium alloy matrix composites and analysed that its behaviour is related on the amount of reinforcement [3, 4]. It is studied that more purpose full factors on mechanical and wear properties of composites are gathered when reinforced with the equal amount of nano-particles than micron sized particles [5, 6]. It is studied that insertion of Al_2O_3 fibres in AM60 Alloy can improve the wear resistance by changing it from mild to severe wear [7]. The composites increase wear resistance with volume fraction improvement, to be clear just 1.11 wt% of nano sized alumina particulates are effective up to 1.8 times increase of pure magnesium [5].

The wear and friction of the composite as well as base alloy mainly depends on certain factors such as applied load, sliding distance, sliding velocity and percentage of reinforcement. This work figures out how these parameters will influence the wear and friction. Taguchi method was used as a soft methodology to identify the influence of these parameters. Experimentation based on design of experiments was done using pin on disk with the counter part of steel investigates the wear and friction properties of AZ91 magnesium alloy and its composites.

Taguchi's efforts are especially in the development of designs for studying variation. Success in achieving the desired results involves a careful selection of process parameters and bifurcate them into control and noise factors. Selection of control factors must be made such that it nullifies the effect of noise factors. Taguchi Method involves identification of proper control factors to obtain the optimum results of the process. The study not only helped in decreasing their number of experiments based on orthogonal arrays but also decreased the cost of experimentation. Taguchi method is also helpful to identify qualitative characteristics using S/N (signal/ Noise) ratios. These qualitative characteristics are 1. Smaller the better, 2. Higher the better, 3. Nominal the best. To analyse the study of friction and wear the smaller the better characteristic is used [2, 8].

2. Materials

AZ91E alloy that has a nominal composition (in weight percent) of 9 Al, 1 Zn, 0.25 Mn and balancing Mg was used as matrix material. 1 to 3 weight percent of alumina (Al_2O_3) powder having an average particle size of 50 nm was used as reinforcement.

3. Fabrication of Composites

Composite preparation is carried out in a crucible made of mild steel in a resistance furnace, Fig. 1(a). A high purity (99.98%) of argon gas along with a cover of flux (20% KCl, 50% $MgCl_2$, 15% MgO, 15% CaF_2, wt. %) is used to prevent oxidation of molten metal. Preheating is done for raw materials, moulds and flux to avoid casting defects. The preheated AZ91E (10 wt% Excess material to compensate Oxidation losses) along with 1% flu is placed in crucible at a temperature of 250^0C and then the temperature is raised to 700^0C and kept constant for about 20 min to get homogenized. The liquidus and solidus temperatures of the AZ91 alloy are found to be 596^0C and 468^0C [9]. So, the melt was slowly cooled down to 590^0C to keep the material in the semisolid condition. After cleaning the surface of the melt, the slurry is stirred. The preheated Al_2O_3 particulates (Avg. size 50 nm) in corresponding wt% wrapped in an aluminum foil is submerged beneath the melt. A mechanical stirrer with four blades, Fig. 1(b) is used to stir the mixture at a rotation speed of 450 rpm for 4 minutes and then poured into a permanent steel mould to form the ingots of 15mm diameter with 150 mm length. Similar procedure is done with different wt% reinforcement of nano-particles.

This two-step processing method extends its ability to break up the gas layer around the particle surface. Generally the particles have a fine layer of gas formed on the surface, which impedes wetting between the particles and molten metals. The high melt viscosity produces more abrasive action on the particle surface which can break the gas layer more effectively when compared to conventional stirring for mixing of particles [10]. It also needs to mention about stir casting process in the entrapment of gasses and unwanted inclusions. Magnesium alloy quickly reacts to oxidation if the gasses and inclusions are entrapped once; the increased viscosity of the vigorously stirred melt obstructs easy elimination of theses detriments.

(a) Melting Furnace with Argon Gas arrangement **(b) Automatic stirrer**

Fig. 1. Stir casting experimental setup.

4. Design of Experiments

The experiments are conducted as per the standard orthogonal array. The selection of the orthogonal array depends up on the condition that the degrees of freedom for the orthogonal array should be greater than or equal to sum of those wear parameters [9]. In the present investigation, an L9 orthogonal array is chosen, which has 9 rows and 4 columns as shown in Table 1. The wear parameters chosen for the experiments are (i) sliding speed (S) (ii) sliding distance (D) , (iii) load (L) and (iv) percentage of reinforcement(R). Table 2, indicates the factors and their level. The experiment consists of 9 tests (each row in the L9 orthogonal array) and the columns are assigned with parameters. The response to be studied is the wear with the objective of smaller is the better [11]. The experiments are conducted as per the orthogonal array with the level of parameters given in each array row.

Table 1. Layout of orthogonal array.

	L9 (34) Orthogonal array				
	Independent Variables				Performance Parameter Value
Experiment #	S	L	D	R	
1	1	1	1	1	p1
2	1	2	2	2	p2
3	1	3	3	3	p3
4	2	1	2	3	p4
5	2	2	3	1	p5
6	2	3	1	2	p6
7	3	1	3	2	p7
8	3	2	1	3	p8
9	3	3	2	1	p9

Table 2. Control factors and their levels.

PARAMETER	Symbol	UNITS	LEVEL 1	LEVEL2	LEVEL 3
Sliding Speed	S	m/sec	1	3	5
Sliding Distance	D	m	500	1000	1500
Applied Load	L	N	10	15	20
%of Reinforcement	R	%	1	2	3

5. Experimental Setup and Procedure

The tests on dry sliding wear are performed using 6mm diameter and 40mm long pin samples machined out from the castings and are shown in Fig. 2. A pin-on-disc machine shown in Fig. 3 (M/s DUCOM, Bangalore, India) with counter face of a hardened and polished disc made of EN-32 steel (HRC 62-65 hardness) was used for the wear tests.

The block diagram shown in Fig. 4 shows the step-by-step procedure used to evaluate the dry sliding wear. The initial weight of the specimen was measured in a single pan electronic weighing machine with least count of 0.001 g. During the test the pin was pressed against the counterpart rotating against EN32 steel disc with hardness of 65 HRC by applying the load. After running through a fixed sliding distance, the specimens were removed, cleaned with acetone, dried and weighed to determine the weight loss due to wear. The difference in the weight measured before and after test gave the dry sliding wear of the composite specimen and then the volume loss was calculated. The wear of the composites was studied as a function of the sliding distance, applied load, percentage of reinforcement and the sliding velocity.

Fig. 2. Wear Specimen machined by EDM

Fig. 3. DUCOM wear and friction machine.

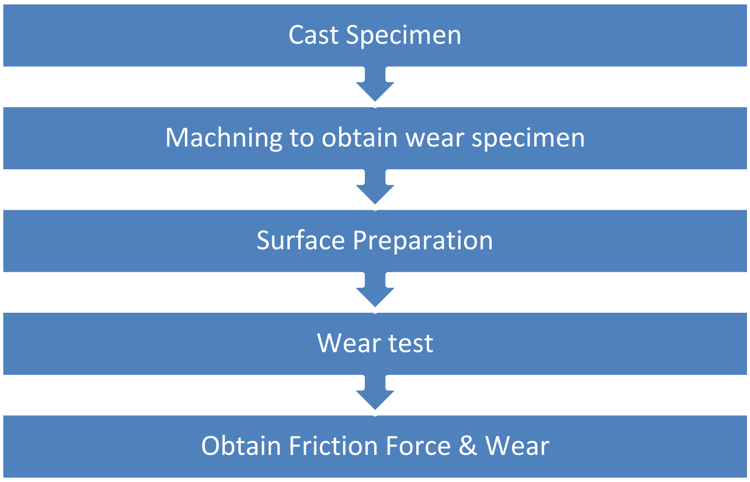

Fig. 4. Step by step procedure used to evaluate the dry sliding wear.

6. Results and Discussions

The influence of control parameters sliding distance, load, sliding speed and reinforcement content on wear and friction have been evaluated using *S/N* ratio response analysis individually. Taguchi recommends the use of signal to noise ratio which estimates the inverse of the coefficient of variation, that is, estimates the ratio μ/σ, with μ being the process mean and σ the process standard deviation.

The wear rate and friction force is considered as the quality characteristic with the concept of "the smaller-the-better" and calculated by using following Eq. (1). Table 1 shows S/N ratio values of wear and friction.

$$S / N ratio = -10 Log_{10}\left[\frac{1}{n}\sum y^2\right] \tag{1}$$

Here *n* is (wear) and *y* is response value (wear value).

Table 3 shows analysis of *S/N* ratios. The optimum quality with minimum variance was achieved by setting the process parameters with highest *S/N* ratio. The difference between the maximum and minimum value of the mean of *S/N* ratios yields the control parameter which is strongly influenced. Higher the difference between the mean of *S/N* ratios, the more influential will be the control parameter.

Influence of each control factor on the wear and friction performance is obtained from the response tables (Table 4 and 5) of mean *S/N* ratio. It indicates the *S/N* ratio at each level of control factor and how it is changed when settings of each control factor is changed at different levels. It is evident from tables that the sliding distance mostly influences the wear and the applied load influences the frictional force.

The control factor with the strongest influence is determined by difference in values of the largest and the smallest of mean *S/N* ratio at different levels. The higher the difference, the more influential the control factor is. Generally, when the signal to noise ratio is higher than the corresponding parameter level it gives optimal performance. The main effect plots of *S/N* ratios corresponding to friction and wear are shown in Figs. 5 and 6.

From Fig. 5 and table 4 load is a dominant parameter on the frictional force and from Fig. 6 and Table 5 Sliding distance is a dominant parameter on the wear. Based on discussions it is also evident from tables that the optimum conditions for wear are *S*: 3m/sec; *L*: 20N; *D*: 1500 m and percentage of reinforcement: 3%. Similarly the optimum conditions for frictional force are S: 1m/sec; *L*: 20N; *D*: 1500 m and percentage of reinforcement: 3%.

Table 3. *S/N* Ratio analysis values.

Test Number	Velocity	Load	Distance	% of Reinf	Wear	Friction	S/N (Wear)	S/N (Friction)
1	1	10	500	1	175	1.9	-44.86	-5.57
2	1	15	1000	2	425	3.2	-52.56	-10.10
3	1	20	1500	3	567	4.3	-55.07	-12.66
4	3	10	1000	3	283	1.9	-49.03	-5.57
5	3	15	1500	1	571	3.1	-55.13	-9.82
6	3	20	500	2	293	2.9	-49.33	-9.24
7	5	10	1500	2	332	1.7	-50.42	-4.60
8	5	15	500	3	278	2.9	-48.88	-9.24
9	5	20	1000	1	416	3.7	-52.38	-11.36

Table 4. *S/N* ratio values by factor level corresponding to friction force.

Level	Load	Velocity	Distance	% of Ref
1	5.25	-9.44	-8.02	-8.92
2	-9.72	-8.21	-9.01	-7.98
3	-11.09	-8.40	-9.03	-9.16
Max-min	5.84	1.23	1.01	1.17
Rank	1	2	3	4

Table 5. *S/N* ratio values by factor level corresponding to wear:

Level	Load	Velocity	Distance	% of Ref
1	-48.10	-50.83	-47.69	-50.79
2	-52.19	-51.16	-51.32	-50.77
3	-52.26	-50.56	-51.32	-50.99
Max-min	4.15	0.60	5.849	0.22
Rank	2	3	1	4

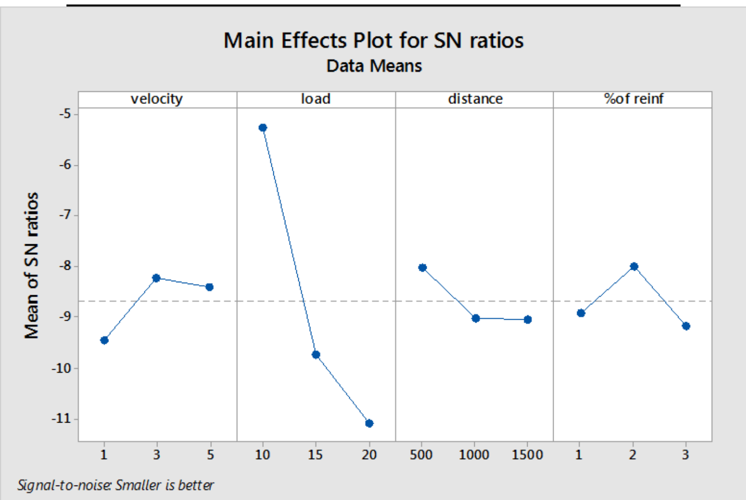

Fig. 5. Main effect plots of S/N ratios for friction force.

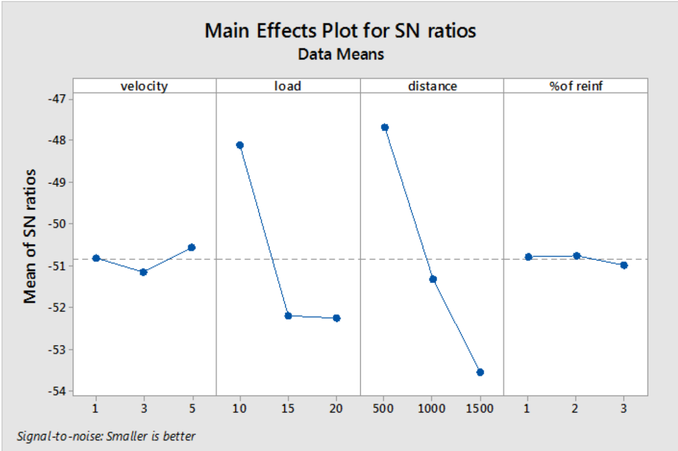

Fig. 6. Main effect plots of S/N ratios for wear.

4.1. Multiple linear regression analysis

A multiple linear regression analysis is utilized to model the relationship between two or more predictor variables and a response variable by curve fitting a linear equation to the observed data. In order to establish the correlation between the wear and friction parameters: sliding Speed (*S*), normal load (*L*), sliding distance (*D*), and percentage of Reinforcement (*R*) the multiple linear regression model was used.

As the relations existing between the wear, friction force with the parameters are exponential in nature [12], we assume

$$Wear = A.\ S^{b1}.\ L^{b2}.\ D^{b3}.\ R^{b4} \quad (2)$$

where A, b_1, b_2, b_3 and b_4 are constants to be determined. If we take logarithm on both sides a much simpler equation is obtained.

$$Log_{10}W = Log_{10}A+b1\ Log_{10}S+b2\ Log_{10}L+b3\ Log_{10}D+b4\ Log_{10}R \quad (3)$$

Similarly for friction force

$$Log_{10}FF = Log_{10}A+c_1\ Log_{10}S+c_2\ Log_{10}L+c_3\ Log_{10}D+c_4\ Log_{10}R \quad (4)$$

So the simplified relations are

$$Y= a+b_1x_1+b_2x_2+b_3x_3+b_4x_4 \quad (5)$$

$$Z= a+c_1x_1+c_2x_2+c_3x_3+c_4x_4 \quad (6)$$

which are the linear equations and we determined the constants by using multiple linear regression.

From analysis we obtained the constants and substituted in Eq. (5) and (6) and the equations are as follows

$$Wear = -67 - 11.8 log_{10} S + 16.20 log_{10} L + 241.3 log_{10} D - 5.7 log_{10} R \quad (7)$$

$$FF = -.181 - 0.0917 \log_{10} S + 0.1800 \log_{10} L + 0.467 \log_{10} D + 0.067 \log_{10} R \quad (8)$$

Finally by substituting the values in to exponential form the wear and friction force equations will be

$$W = 10^{-67.} S^{-11.8}. L^{16.2}. D^{241.3}. R^{-5.7} \quad (9)$$

$$FF= 10^{-0.181}. S^{-0.0917}. L^{0.18}. D^{0.467}. R^{0.067} \quad (10)$$

Equations (9) and (10) show the regression equations for wear and friction force respectively. In this study, results obtained from wear and friction are in good agreement with regression models (R^2=0.942). It can be noted that since the value of regression coefficient for the model is 0.942, the wear data were not scattered. Since both the values are reasonably close to unity, models provide a reasonably good explanation of the relationship between the independent factors and the response.

It can be observed from equation 6 that the coefficient associated with sliding Speed (*S*) and percentage of reinforcement (*R*) is negative. It indicates that the wear of the material decreases with increase in sliding speed and percentage of reinforcement. Conversely the wear rate of the material increases with increase in applied load (*L*) and sliding distance (*D*) since the coefficient associated with the applied load and sliding distance are positive. Similarly from equation II the coefficient associated with sliding Speed (*S*) is negative. It indicates that the frictional force decreases with increase in sliding speed and increases with increase in other three parameters.

4.2. Morphology of wear surfaces:

The SEM analysis of wear surfaces of 2% reinforcement with 10 N and 20 N of applied load is shown in the Figs. 7 and 8, as it is showing the good wear tracks and plastic deformation of material. It reveals that particulate reinforcement plays an important role in increase of wear rate.

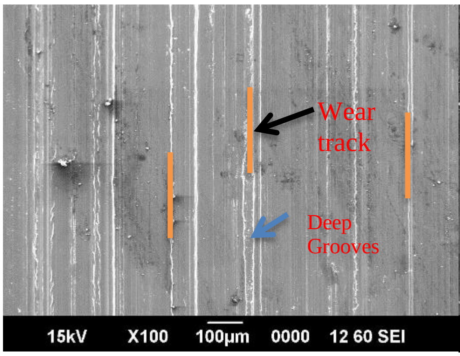

Fig. 7. SEM micrograph of specimen with 2% reinforcement tested at a velocity of 5m/s and a distance of 1.5 KM at 20 N load.

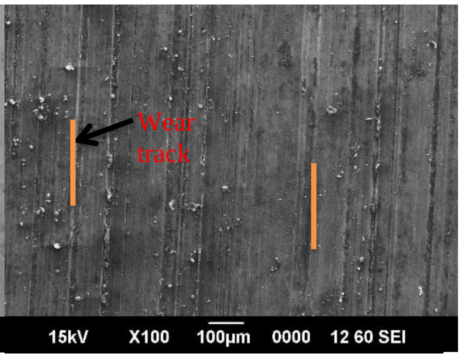

Fig. 8. SEM micrograph of specimen with 2% reinforcement tested at a velocity of 5m/s and a distance of 1.5 KM at 10N load.

The white patches shows the plastic flow of the material, and it is due to the frictional heat generated at the sliding surface. It shows smoother surfaces at lower normal loading condition. In these figures, we can find difference in the height of wear track which may be due to direct contact of reinforcement material with the disc. Fig. 7, which is at higher normal load that shows some distortion and more plastic flow of material. The straight lines show the directional path of wear.

7. Conclusions

In the present work, AZ91E/nano-Al_2O_3 Mg-MMCs were prepared by the semi-solid stir casting process and the influence of various parameters on dry sliding wear properties was investigated. The following are the conclusions observed from present investigation

- The AZ91E/ Al_2O_3 composites have been successfully produced by the two step stir casting route for study on the mechanical and tribological properties.
- The reinforcement particles play a prominent role in enhanced wear resistance of the composites. It was found that the transition load increases with an increase in reinforcement content and the wear rate of the composite was lower than that of the base alloy.
- Dry sliding wear characteristics of these composites can be successfully analysed using taguchi technique. This method provides a simple, systematic and efficient methodology for the optimization of control factors.
- Based on S/N ratios it is concluded that sliding distance and load are the factors that have the highest physical as well as statistical influence on the wear and friction respectively.
- A multiple linear regression model was developed to predict the wear rate of the composites. The closeness of the results of predictions based on calculated S/N ratios and experimental values show that the Taguchi experimental design technique can be used successfully for both optimization and prediction.

References

1. Kumar, D.S.; Tarasasanka, C.; Ravindra, K.; and Suman, K.N.S. (2015). Magnesium and its alloys in automotive applications – A review. *American Journal of Materials Science and Technology*, 4(1), 12-30.
2. Girish, B.M.; Satish, B.M.; Sarapure, Sadanand.; Somashekar, D.R.; and Basawaraj (2015). Wear behavior of magnesium alloy AZ91 hybrid composite materials. *Tribology Transactions*, 58(3), 481-489.
3. Lim, C.Y.H.; Lim, S.C.; and Gupta, M.; (2003). Wear behaviour of SiCp-reinforced magnesium matrix composites. *Wear*, 255(1-6), 629-637.
4. Yao, J.; Li, W.; Zhang, L.; Wang, F.; Xue, M.; Jiang, H.; and Lu, J. (2010). Wear mechanism for in situ TiC particle reinforced AZ91 magnesium matrix composites. *Tribology Letters*, 38(3), 253-257.
5. Lim, C.Y.H.; Leo, D.K.; Ang, J.J.S.; and Gupta, M.; (2005). Wear of magnesium composites reinforced with nano-sized alumina particulates. *Wear*, 259(1-6),620-625.
6. Cao, G.; Konishi, H.; and Li, X. (2008). Recent developments on ultrasonic cavitation based solidification processing of bulk magnesium nanocomposites. *International Journal of Metallurgy*, 2(1) ,57-65.
7. Banerji, A.; Hu, H.; and Alpas, A.T. (2012). Ultra-mild wear of Al_2O_3 fibre and particle reinforced magnesium matrix composites. *Advanced Material Research*, 445, 503-508.
8. Sivarao,S.; Milkey, K.R.; Samsudin, A.R.; Dubey, A.K.; and Kidd, P. (2014). Comparison between Taguchi method and Response Surface Methodology

(RSM) in modelling CO_2 laser machining. *Jordan Journal of Mechanical and Industrial Engineering*, 8 (1), 35-42.

9. Poddar, P.; Mukherjee, S.; and Sahoo, K.L. (2009). The microstructure and mechanical properties of SiC reinforced magnesium based composites by rheocasting process. *Journal of Materials Engineering & Performance*, 18(7), 849-855.
10. Ameen, H.A; Hassan, K.S.; and Mubarak, E.M.M. (2011). Effect of loads, sliding speeds and times on the wear rate for different materials. *American Journal Of Scientific And Industrial Research*, 2(1),99-106.
11. Basavarajappa,S.; Chandramohan, G.; and Paulo Davim, J. (2007). Application of Taguchi techniques to study dry sliding wear behaviour of metal matrix composites. *Material Design*, 28(4), 1393-1398.
12. Mukherjee, S.N. and Basu. S.K. (1967). Multiple regression Analysis in Evaluation of Tool wear. *International Journal of Machine Tool Design and Research*, 7(1), 15-21.